A Robust Continuous-Time Multi-Dithering Technique for Laser Communications using Adaptive Optics

Dimitrios N. Loizos
Electrical and Computer Engineering
The Johns Hopkins University
Baltimore, MD 21218
dloizos@jhu.edu

Paul P. Sotiriadis
Electrical and Computer Engineering
The Johns Hopkins University
Baltimore, MD 21218
pps@jhu.edu

Gert Cauwenberghs
Division of Biological Sciences
University of California, San Diego
San Diego, CA 92093
gert@ucsd.edu

Abstract—A robust system architecture to achieve optical coherency in multiple-beam free-space laser communication links with adaptive optics is introduced. It is based on deterministic multi-dithering and gradient descent flows and accounts for phase delays in the dither signal, during propagation in the atmosphere, as well as saturation of the optical phase shifters. The architecture has been mathematically analyzed and simulation results of a VLSI implementation of the architecture are presented and found in agreement with the theoretical model.

I. INTRODUCTION

The inherent property of high carrier frequency characterizing laser communications has always been one of their major advantages over conventional RF communications, as it provides a larger modulation bandwidth and therefore higher data rates, and less interference between optical systems. The reason that laser communications have not expanded as expected, so far, has been the difficulty to compensate for atmospheric turbulence. Turbulence causes random optical inhomogeneities in the atmosphere that result in beam spreading, beam wander and scintillation (intensity fluctuation), and therefore distort the transmitted data [1].

Over the last few decades, significant work has been done in the field of adaptive optics in order to alleviate or at least mitigate wave-front distortion and therefore enhance the use of laser communication systems. The techniques that have been so far proposed can be divided into two main categories [2]: wave-front conjugation and model-free optimization. Wave-front conjugation requires the reconstruction of the wave-front at the receiver and provides information for both phase distortion and amplitude modulation [3]. Model-free optimization techniques are computationally simpler and focus on optimizing a system performance metric with respect to phase, without any knowledge of the propagation path [2], [4], [5]. This is usually done by superimposing a perturbation to a control signal and calculating the gradient of the metric.

Although the wave-front conjugation technique has the advantage of being able to derive the additional information of amplitude modulation, phase-only correction of the wave-front is theoretically sufficient for a propagation distance in the near field, and has been also demonstrated to provide significant improvement in the transmitted beam quality for large distance optical communications [6]. Most of the adaptive optics techniques nowadays use phase-only correction for the wave-front control. Moreover, under conditions of strong intensity modulation used in several laser communication schemes, the wave-front can be difficultly reproduced, imposing constraints in the use of the wave-front conjugation technique [5].

The factors discussed above, as well as the emergence of high-bandwidth phase controllers (e.g. [7]) that make possible small high-frequency phase perturbations of the transmitted beam, have shifted the research interest in adaptive optics techniques towards model-free optimization. Several methods that had been proposed in the past, such as multi-dithering [4] and sequential perturbations [8], as well as the recently proposed stochastic parallel gradient descent [5] and decoupled stochastic parallel gradient descent [2] methods seem very promising and can potentially enhance the quality of laser communications.

The purpose of the present work is to propose a system architecture that can implement the multi-dither algorithm for adaptive optics robustly and in continuous-time. Similar architectures have been proposed in the past ([4], [9], [10]), however the one proposed here features several properties that make it attractive for use in modern laser communications. First, it is meant for implementation in a VLSI circuit, combining low-power consumption, compact size, faster computation, higher perturbation frequencies and control of multiple channels. Second, it compensates for possible phase shifts of the dither signal in the case of long-distance communications. Finally, it accounts for saturation of the phase controllers when the multi-dither algorithm dictates continuous increase or decrease in the controlling phase.

II. THE MULTI-DITHER ALGORITHM

The purpose of the multi-dither algorithm is to maximize the value of a performance metric of the optical system, usually the wave-front's intensity. This is done by calculating the gradient of the metric and then, using the gradient descent method, find its maximum value. First, a brief overview of the gradient descent method is given and then the mathematical approach to the multi-dither algorithm is presented.

A. The gradient descent method

Consider the real vector $\mathbf{u} = (u_1, u_2, \ldots, u_n)^{\mathrm{T}}$ and a scalar cost function $J(\mathbf{u})$. The basic form of the gradient descent method is expressed by equation (1) where ϵ is a positive constant and $\mathbf{u}$ evolves in time according to the differential equation (gradient flow)

$$\frac{d\mathbf{u}}{dt} = -\epsilon \nabla J(\mathbf{u}) \tag{1}$$

Taking the derivative of $J(\mathbf{u}(t))$ with respect to time gives

$$\frac{d}{dt} J(\mathbf{u}(t)) = \left(\nabla J(\mathbf{u}) \right)^{\mathrm{T}} \frac{d\mathbf{u}}{dt} = -\epsilon \| \nabla J(\mathbf{u}) \|^2 \tag{2}$$

indicating that $J(\mathbf{u}(t))$ is a strictly decreasing function of time unless $\mathbf{u}$ has reached an equilibrium point of (1).

Assuming that J does not have saddle points, (2) implies that the gradient flow (1) reaches a (local) minimum of J. By flipping the sign of ϵ, we get the gradient flow $d\mathbf{u}/dt = \epsilon \nabla J(\mathbf{u})$ that reaches a (local) maximum of J.

A variation of (1) having practical advantages is derived by keeping only the *sign* information of the partial derivatives in $\nabla J(\mathbf{u})$, i.e.

$$\frac{d\mathbf{u}}{dt} = -\epsilon \operatorname{sgn}\big(\nabla J(\mathbf{u})\big) \tag{3}$$

where the sgn function is applied element-wise to vector $\nabla J(\mathbf{u})$. Following similar steps as before we get that

$$\frac{d}{dt}J(\mathbf{u}(t)) = \big(\nabla J(\mathbf{u})\big)^{\mathrm{T}}\frac{d\mathbf{u}}{dt} = -\epsilon \sum_{i=1}^{n}\left|\frac{\partial J}{\partial u_i}\right| \tag{4}$$

which leads to the same qualitative behavior as (1) but requires much simpler, ± 1, control signals.

B. Sinusoidal multi-dithering

In order to converge to the local (global) minimum/maximum, the gradient descent/ascent method needs the information of the gradient's value for metric J. In our approach, this is provided through the multi-dither algorithm. Let n be the size of vector $\mathbf{u}$, that represents the control signals of the phase controllers. In the (deterministic) *sinusoidal multi-dithering method*, sinusoidal dithers of different frequency for each element (channel) of vector $\mathbf{u}$, are superimposed to the control $\mathbf{u}$

$$\tilde{\mathbf{u}} = \mathbf{u} + \boldsymbol{\theta} = \mathbf{u} + \alpha\left[\cos(\omega_1 t), \cos(\omega_2 t), \ldots, \cos(\omega_n t)\right]^{\mathrm{T}} \tag{5}$$

where α is a small scalar parameter. Evaluating J using Taylor series we get that

$$\begin{aligned}
J(\tilde{\mathbf{u}}) = J(\mathbf{u} + \boldsymbol{\theta}) \quad &= J(\mathbf{u}) + \big(\nabla J(\mathbf{u})\big)^{\mathrm{T}}\boldsymbol{\theta} + \ldots \\
&= J(\mathbf{u}) + \alpha \sum_{i=1}^{n}\left.\frac{\partial J}{\partial u_i}\right|_{\mathbf{u}}\cos(\omega_i t) + \ldots
\end{aligned} \tag{6}$$

To extract the entries of the gradient vector $\nabla J(\mathbf{u})$ we first multiply $J(\tilde{\mathbf{u}})$ with $\cos(\omega_j t)$, $j = 1, 2, \ldots, n$. This gives

$$\begin{aligned}
J(\tilde{\mathbf{u}})\cos(\omega_j t) \quad = \quad & J(\mathbf{u})\cos(\omega_j t) \\
& +\frac{\alpha}{2}\left.\frac{\partial J}{\partial u_j}\right|_{\mathbf{u}} + \frac{\alpha}{2}\left.\frac{\partial J}{\partial u_j}\right|_{\mathbf{u}}\cos(2\omega_j t) \\
& +\frac{\alpha}{2}\sum_{i\neq j}\left.\frac{\partial J}{\partial u_i}\right|_{\mathbf{u}}\cos\big((\omega_i - \omega_j)t\big) \\
& +\frac{\alpha}{2}\sum_{i\neq j}\left.\frac{\partial J}{\partial u_i}\right|_{\mathbf{u}}\cos\big((\omega_i + \omega_j)t\big) \\
& + \text{H.O.T.}
\end{aligned} \tag{7}$$

Note that there is only one constant term on the right hand side of (7). Assuming that the frequency differences $(\omega_i - \omega_j)$, $i \neq j$ are not very small, passing signal (7) through a low pass filter gives

$$\overline{J(\tilde{\mathbf{u}})\cos(\omega_j t)} = \frac{\alpha}{2}\left.\frac{\partial J}{\partial u_j}\right|_{\mathbf{u}}. \tag{8}$$

(where over-line means low-passing). This process is performed in parallel for all channels, $j = 1, 2, \ldots, n$, and in this way the gradient of J is reconstructed.

The above analysis indicates that both the dither frequencies, ω_j, as well as the dither frequency differences $\omega_i - \omega_j$, $i \neq j$ should be larger than the bandwidth of the low-pass filter, in order to avoid crosstalk between the dithering signals of the channels.

Expression (8) was derived with the implicit assumption that the detection is synchronous, i.e. zero phase difference between the *cosines*. In reality however, the phases of the perturbation signals are delayed by $\varphi_i = \omega_i T$ where T is a summation of several propagation delays and processing times: the time the laser beam travels from the transmitter to the receiver, the processing time it takes the receiver to estimate the instantaneous power and transmit it back to the phase controller, the time the feedback signal travels from the receiver to the phase controller at the transmitter, plus any delay due to processing in the phase controller's module. By taking this into account we get

$$\overline{J(\tilde{\mathbf{u}})|_{T-delay}\cos(\omega_j t)} = \frac{\alpha}{2}\left.\frac{\partial J}{\partial u_j}\right|_{\mathbf{u}}\cos(\varphi_j). \tag{9}$$

Combining the above multi-dithering approach for estimating the gradient vector with the modified gradient descent, (3), we get

$$\frac{d\mathbf{u}}{dt} = \epsilon \operatorname{sgn}\left(\left[\overline{J(\tilde{\mathbf{u}})|_{T-delay}\cos(\omega_j t)}\right]_{j=1}^{n}\right) \tag{10}$$

The sign of ϵ was flipped since we want to maximize J. Note that $\cos(\varphi_j)$ does not influence the result as long as the delay corresponds to less than $90°$ phase shift. The proposed system architecture described in the next Section is able to compensate for larger phase shifts.

Written in a more compact way, equation (10) can take the form

$$\frac{d\mathbf{u}}{dt} = \epsilon \operatorname{sgn}\big(\nabla J\big(\mathbf{u}(t - T)\big)\big) \tag{11}$$

III. SYSTEM ARCHITECTURE

The configuration of the overall optical communication system is shown in Fig. 1. A modulated high power laser beam is split
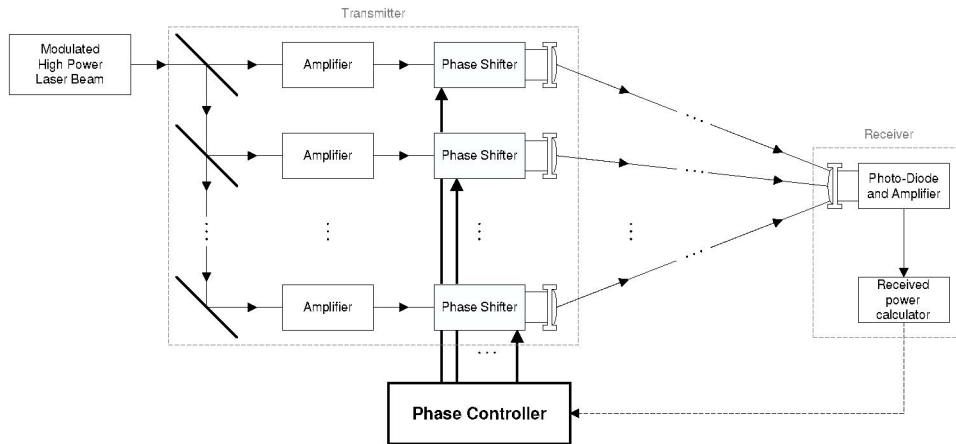

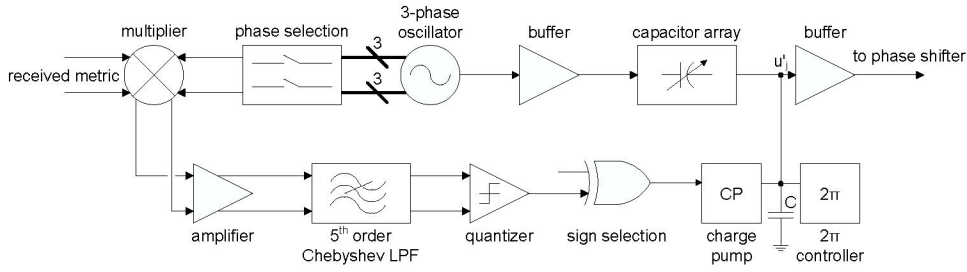Fig. 1.   Optical system configuration

Fig. 2. Block diagram for one channel of the phase controller

into n different channels. The beams at each channel are amplified and then phase shifted according to the controls provided by the phase controller. Each beam follows a different path through the atmosphere, that is considered of unknown properties. The wavefront at the receiver is a combination of the wave-fronts from all channels and its intensity is detected through a photodiode. The desired performance metric is calculated and the information of its value is transmitted back to the phase controller. The phase controller calculates the appropriate phase shifts that maximize the metric and adjusts the control of the phase shifters, closing the feedback loop.

The purpose of this work, as mentioned above, is to present a system architecture for the phase controller. The phase controller can control multiple channels. In Fig. 2, the system architecture for channel j, $j = 1 \ldots n$ is shown. The control $\mathbf{u}'$, that adjusts the phase shifters, constitutes of two components: a slow-varying one provided by the charge pump, and a high-frequency small amplitude dither coming from the oscillator. The amplitude of the dither is set by appropriately adjusting the ratio between C and the capacitance of the capacitor array. The signal $\mathbf{u}'$ controls the phase alteration of the transmitted laser beam from this channel.

After the performance metric J has been computed in the receiver, and the information of its value has been transmitted to the phase controller, synchronous detection is performed at every channel, as dictated by (7). The phase selection attribute will be discussed later. After the metric and the oscillator's signal have been multiplied in channel j, the output is low-passed by a 5th order Chebyshev filter, that features sharp cutoff and low ripple in the bandpass. According to the analysis of Section II, this lowpass filtering should provide us with the partial derivative of J with respect to u_j. This information is enough to perform gradient descent maximization. However, we have chosen to quantize this partial derivative and retrieve only the sign information for reasons that will be explained later. A controllable charge pump, then, scales the magnitude of the sign information (the ϵ used in Section II) and updates the voltage on capacitor C.

The 2π controller compares the value of control u'_j with an upper and lower threshold. These thresholds indicate the upper and lower limits that the controls $\mathbf{u}$ of the phase shifters can take before the phase shifters saturate. If u'_j exceeds or drops below these thresholds, the voltage on capacitor C is instantaneously set to a predefined value. The voltage drop or jump on the capacitor and therefore on u'_j corresponds to a 2π phase shift on the phase shifter. Therefore, the phase shifters are effectively driven away from saturation without any impact on the instantaneous phase shift added to each channel.

A. Phase selection

As was discussed in Section II, in the case where the atmospheric path introduces a phase delay greater than $90°$ to the perturbation, synchronous detection might fail, giving a signal whose sign is opposite to what we would expect. To compensate for this, a 3-phase oscillator (phases at $0°$, $120°$ and $240°$) is proposed to be used in the architecture, giving the flexibility to choose the phase of the oscillator closest to that of the perturbation after propagating through the atmospheric medium. An additional degree of freedom for choosing the phase is given by the sign selection block (Fig. 2). Graphically, this can be represented as a division of the phase domain into 6 equally sized subdomains (Fig. 3). Depending on the phase delay of the perturbation, the appropriate phase of the oscillator and the correct sign can be selected so that the phase subdomain where the phase delay lies on is chosen. At this point it is worth mentioning that the sign selection block (Fig. 2) gives also the possibility of performing minimization instead of maximization of the performance metric, if this is required.
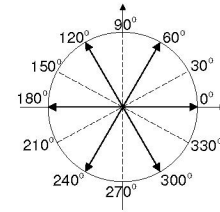

Fig. 3. Phase domain - the dashed lines represent the boundaries of the subdomains and the bold lines the selected phase for the synchronous detector at these subdomains

B. Quantization

Instead of using directly the gradient of J, it is proposed to use only the information of its sign, provided by the quantization of the lowpass filter's output. As mentioned in Section II, this information is sufficient to perform the gradient descent algorithm. Moreover, given that the correct phase subdomain has been selected, this information is independent of any phase offset φ_i between the perturbation of the metric and the selected phase of the oscillator. However, the choice of keeping only the sign information of the gradient was mainly made for issues of stability of the feedback system.
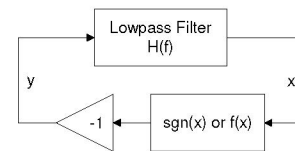

Fig. 4. Simplified closed loop diagram for the feedback of each channel

Consider the feedback loop for each channel which can be reduced to the system of Fig. 4. Assuming that the lowpass filter $H(f)$ has
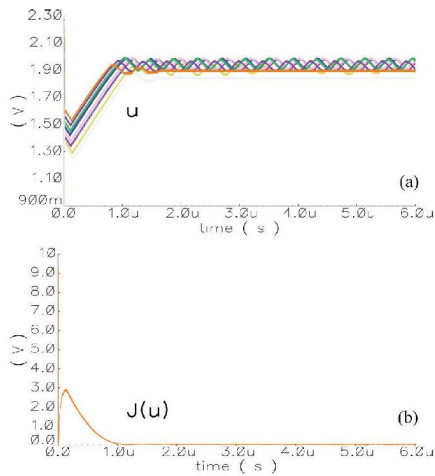
Fig. 5. Simulation results for perturbation frequencies between 100-800MHz and high gain in the charge pump

Fig. 6. Simulation results for perturbation frequencies between 100-800MHz and low gain in the charge pump

at least two poles, the closed system will potentially oscillate at the frequency at which the Barkhausen phase criterion for oscillation is satisfied, i.e. when the phase response of the filter reaches 180°. For the system to indeed oscillate, the Barkhausen amplitude criterion for oscillation needs to be also satisfied. In the case where a limiter function is used in the closed loop, the criterion is always satisfied and the loop will always oscillate. However, the amplitude of oscillation is controllable by adjusting the bounds of the limiting function. If, on the other hand, a linear feedback is used, the system can potentially be made stable, if all the gains and phase responses of the system are known. Nonetheless, it may not be easy to predict these gains. Moreover, if the system starts oscillating, the amplitude of oscillation will be limited only by the non-linearities of the components.

IV. SIMULATION RESULTS

The proposed architecture with 8 control channels has been designed in a 0.5μm SiGe technology. The design of the channels has been done in such a way so that the oscillation frequency and the cutoff frequency of the lowpass filters are tunable over at least 3 decades. Some preliminary simulation results are presented that prove the validity of the architecture. Simulations were performed for the case of minimization of the performance metric, but as discussed earlier, the system can also perform maximization by appropriately controlling the sign selection signal (Fig. 2).

A first simulation was conducted with perturbation frequencies for the 8 channels between 100-800MHz and steps of 100MHz, and a performance metric to be minimized $J(\mathbf{u}) = \sum_{i=1}^{8}(u_i - 2)^2$. The cutoff frequency of the lowpass filters was set to 10MHz. Fig. 5(b) demonstrates how the metric is minimized, while Fig. 5(a) shows the expected oscillation of the controlling signals u_i, $i = 1\ldots 8$, around the expected value of 2V, after convergence. A limit cycle of amplitude around 100mV can be observed for the signals u_i, due to the high gain (parameter ϵ in Section II) that had been selected for the charge pump. Convergence is achieved in almost 1μs.

A second simulation with the exact same setup as the first one but with a considerably lower gain for the charge pump was run. Fig. 6(a) shows that the amplitude of the limit cycle dropped, to a point that is practically negligible, while Fig. 6(b), demonstrates that the convergence time increased, indicating a trade-off between the convergence time of the system and the amplitude of the limit cycle.
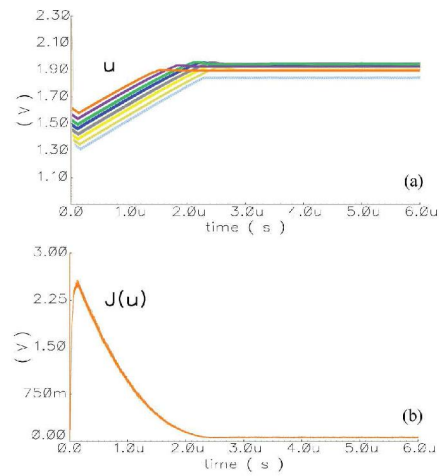
Similar conclusions have been derived by simulations of the system at frequencies in the range between 100 and 800kHz.

V. CONCLUSION

A system architecture implementing a multi-dithering algorithm with gradient descent for adaptive optics has been described and analyzed. The architecture compensates for phase delays and saturation of the controlled optical phase shifters. The system is capable of minimizing or maximizing the performance metric and the gradient descent optimization is achieved using only the sign information of the gradient. Simulation results of a VLSI implementation in SiGe technology have been presented and demonstrate the validity of the architecture.

REFERENCES

[1] T. Weyrauch and M.A. Vorontsov, "Free-space laser communications with adaptive optics: Atmospheric compensation experiments," *J. Opt. Fiber Commun. Rep.*, 2004, pp. 355-379.

[2] M.A. Vorontsov, "Decoupled stochastic parallel gradient descent optimization for adaptive optics: integrated approach for wave-front sensor information fusion," *J. Opt. Soc. Am. A*, February 2002, Vol. 19, No. 2, pp. 356-368.

[3] M.D. Levenson, "High-resolution imaging by wave-front conjugation," *Optics Letters*, May 1980, Vol. 5, No. 5, pp. 182-184.

[4] T.R. O'Meara, "The multidither principle in adaptive optics," *J. Opt. Soc. Am.*, March 1977, Vol. 67, No. 3, pp. 306-315.

[5] M.A. Vorontsov, G.W. Carhart, M. Cohen and G. Cauwenberghs, "Adaptive optics based on analog parallel stochastic optimization: analysis and experimental demonstration," *J. Opt. Soc. Am. A*, August 2000, Vol. 17, No. 8, pp. 1440-1453.

[6] B.M. Levine, E.A. Martinsen, A. Wirth, A. Jankevics, M. Toledo-Quinones, F. Landers and T.L. Bruno, "Horizontal line-of-sight turbulence over near-ground paths and implications for adaptive optics corrections in laser communications," *Applied Optics*, 20 July 1998, Vol. 37, No. 21, pp. 4553-4560.

[7] T. Bifano, J. Perreault, P. Bierden and C. Dimas, "Micromachined Deformable Mirrors for Adaptive Optics," *Proc. SPIE*, 2002, Vol. 4825, pp. 10-13.

[8] J.W. Hardy, "Active Optics: A New Technology for the Control of Light," *Proc. IEEE*, June 1978, Vol. 66, No. 6, pp. 651-697.

[9] W.B. Bridges, P.T. Brunner, S.P. Lazzara, T.A. Nussmeier, T.R. O'Meara, J.A. Sanguinet and W.P. Brown, Jr., "Coherent Optical Adaptive Techniques," *Applied Optics*, February 1974, Vol. 13, No. 2, pp. 291-300.

[10] J.E. Pearson, W.B. Bridges, S. Hansen, T.A. Nussmeier and M.E. Pedinoff, "Coherent optical adaptive techniques: design and performance of an 18-element visible multidither COAT system," *Applied Optics*, March 1976, Vol. 15, No. 3, pp. 611-621.